BJR

https://doi.org/10.1259/bjr.20210738

Received: 16 June 2021 | Revised: 02 December 2021 | Accepted: 13 December 2021 | Published online: 24 December 2021

Cite this article as:
Lim K, Kwon H, Cho J, Kim D, Kang E, Kim S. Added value of enhanced CT on LR-3 and LR-4 observation of Gd-EOB-DTPA MRI for the diagnosis of HCC: are CT and MR washout features interchangeable?. *Br J Radiol* (2022) 10.1259/bjr.20210738.

FULL PAPER

Added value of enhanced CT on LR-3 and LR-4 observation of Gd-EOB-DTPA MRI for the diagnosis of HCC: are CT and MR washout features interchangeable?

KYUNGJAE LIM, HEEJIN KWON, JINHAN CHO, DONGWON KIM, EUNJU KANG and SANGHYEON KIM

Department of Radiology, Dong-A university Hospital, Dongdaesindong 3ga, Seo-gu, Pusan, South Korea

Address correspondence to: Heejin Kwon
E-mail: *risual@dau.ac.kr*

Objective: To characterize the use of portal venous or delayed phase CT as an alternative to estimate washout for the non-invasive diagnosis of hepatocellular carcinoma (HCC) on gadoxetic acid-enhanced MRI in combination with other features.
Methods: This retrospective study included 226 observations (n = 162 patients) at high risk for HCC imaged with gadoxetic acid-enhanced MRI and enhanced liver CT between March 2015 and March 2018. Two radiologists independently evaluated two sets of images and assigned the final Liver Imaging Reporting and Data System (LI-RADS) categories by consensus using gadoxetic acid-enhanced MRI. LR-1, LR-2, LR-5, and LR-M were excluded from the study.
The observations were divided using different criteria for washout: hypointensity on the portal venous phase (PVP) at MRI (criteria 1), hypointensity on PVP at MRI and/or hypoattenuation on the PVP/delayed phase at dynamic CT (criteria 2), and hypointensity on the PVP and/or hepatobiliary phase at MRI (criteria 3). The sensitivity, specificity, and accuracy for the diagnosis of HCC were analyzed for each criterion.
Results: Using gadoxetic acid-enhanced, 226 lesions were diagnosed as LR-3 or LR-4 by LI-RADS. Among them, 98 and 152 had "washout" at criteria 1 and 2, respectively. For the diagnosis of HCC, criteria 2 and 3 showed significantly higher sensitivities (67.3 and 92.5%, respectively) compared with criteria 1 (35.5%) (p < 0.001). The specificity of criteria 3 (13%) was significantly lower than those of criteria 1 and 2 (40.7% and 38.4%, respectively, p < 0.001). The specificities between criteria 1 and 2 were not statistically different (p = 0.427).
Conclusion: Although the LI-RADS lexicon does not permit the interchange of image features among various image modalities, the sensitivity of HCC diagnosis could be improved without any decrease in specificity by adding CT image washout features.
Advances in knowledge: Although the LI-RADS lexicon does not permit the interchange of image features among various image modalities, complementary use of dynamic CT in LR-3 or LR-4 categories on the basis of gadoxetic acid-enhanced MRI may contribute to major imaging feature.

INTRODUCTION

Hepatocellular carcinoma (HCC) is the most common type of primary liver cancer in adults and is the most common cause of mortality in cirrhotic patients.[1] In 2011, the American College of Radiology introduced the Liver Imaging Reporting and Data System (LI-RADS) to standardize the acquisition, interpretation, and reporting of liver lesions in patients at high risk of HCC. The most updatedLI-RADS v. 2018 includes five major categories (LR-1 to LR-5) based on imaging observations that reflect the relative probability of being benign or HCC.[2] When determining a LI-RADS category, five major imaging features are considered [arterial phase hyperenhancement (APHE), washout appearance, enhancing capsule appearance, size, and threshold growth]. Ancillary features are additional imaging features designed to improve detection and increase reliability. The recent LI-RADS guidelines can be used with various imaging modalities such as dynamic CT, dynamic MRI with extracellular agents, dynamic MRI with hepatocyte-specific agents (*e.g.* gadoxetate disodium), and contrast-enhanced ultrasound.[3,4]

Although LI-RADS represents the relative probability of HCC, it also states that washout features should be interpreted only in the portal venous phase (PVP) to obtain the highest specificity if gadoxetic acid is administered.[5]

Thus, hypointensity in the transitional phase (TP) (which occurs approximately 2–5 min after the injection of gadoxetate disodium and corresponds temporally to the delayed phase after injecting extracellular space agents) does not qualify as washout because of the relative increased uptake of contrast by hepatocytes and reduced retention in any non-hepatocyte lesion. Problematically, indeterminate lesions are commonly encountered during the interpretation of non-washout appearance of HCC in the portal phase using gadoxetic acid-enhanced MRI. According to a previous study,[6] there is a concern about lowering specificity as a trade-off for increasing sensitivity when using hepatobiliary phase (HBP) hypointensity as an alternative to washout PVP.

Focusing on the fact that a large number of patients scanned by dynamic CT before MRI, we aimed to: (i) compare washout on CT and washout on gadoxetic acid-enhanced MRI, (ii) evaluate whether CT provides additional support for the diagnosis of HCC, and (iii) determine whether HBP hypointensity can replace washout.

This study evaluated the added value of washout appearance on CT for indeterminate observations (LR-3 and LR-4) determined using gadoxetic acid-enhanced MRI.

METHODS AND MATERIALS

Our institutional review board approved this retrospective study and waived the requirement for informed consent due to the retrospective nature of the study.

Study population

We retrospectively searched consecutive patients who underwent gadoxetic acid-enhanced MRI and dynamic liver CT less than 2 weeks apart between March 2015 and March 2018. The inclusion criteria were as follows: (i) patients with liver cirrhosis who underwent liver MRI and CT for HCC surveillance and (ii) patients confirmed to have HCC or benign lesions through pathological diagnosis or subsequent imaging over 2 years. The exclusion criteria were as follows: (i) patients with no lesions or only observations difficult to characterize because of small lesion size (<5 mm) or suboptimal image quality (including transient severe motion during arterial phase), (ii) patients with only

Figure 1. Study flowchart. HCC, hepatocellular carcinoma; LI-RADS, Liver Imaging Reporting and Data System.

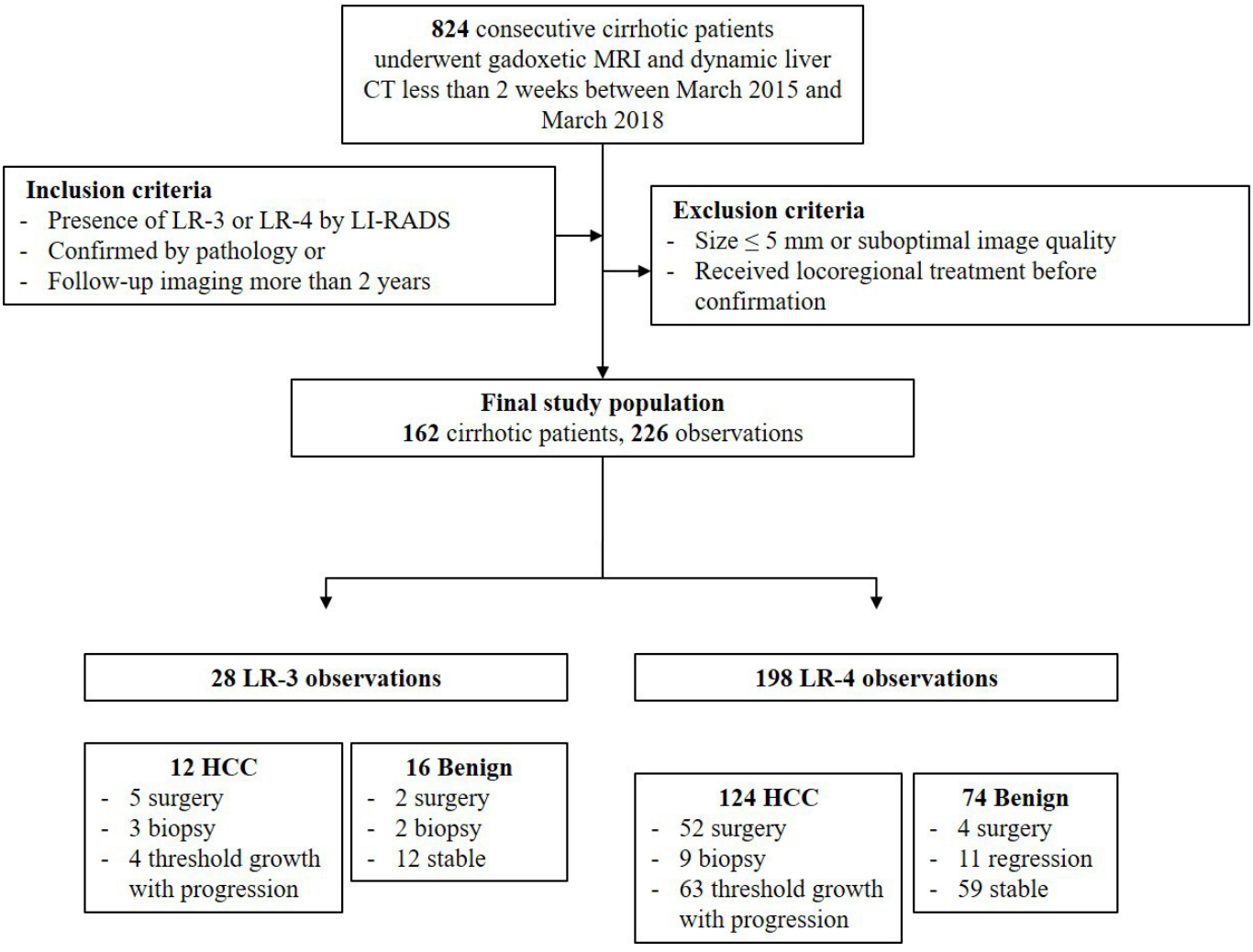

typical benign observations (*e.g.* LR-1 or LR-2), and (iii) patients with LR-5, LR-M, and LR-TIV observations. Figure 1 shows detail of flowchart.

MRI technique

Liver MRI was performed on a 3.0-Tesla system (Discovery MR750, GE Healthcare, Waukesha, WI) with the following sequences included: the localizer images using T_2 weighted single-shot fast spin-echo sequence and chemical shift images using three-dimensional (3D) dual-echo T_1 weighted gradient-echo sequence. Dynamic contrast-enhanced (DCE) images were acquired with a 15 s breath-holding interval before and after contrast agent injection using a 3D-spoiled gradient-echo sequence with two-point Dixon water–fat separation (3D LAVA-FLEX®). Contrast administration was performed at a dose of 0.1 ml/kg of gadoxetic acid (Primovist; Bayer Healthcare) at a rate of 1 ml s^{-1} followed by 20 ml saline flush at the same rate. DCE fat-suppressed 3D T_1 weighted sequences were obtained using liver acquisition with volume acceleration (LAVA; GE Healthcare). Before and after the administration of gadoxetic acid, dynamic T_1 weighted unenhanced, early arterial phase (10s), late arterial phase (35s), PVP (60s), TP (3 min), and HBP (20 min) images (slice thickness, 5 mm; spacing between slice, 2.5 mm) were acquired.

T_2 weighted images and diffusion-weighted images (DWIs) were successively obtained using navigator triggering during the long interval between the TP and HBP. T_2 weighted images were obtained using fat-saturated T_2 weighted turbo spin-echo, known as periodically rotated overlapping parallel lines with enhanced reconstruction, and DWIs were obtained at three b-values (50, 400, 800 s/mm^2). The apparent diffusion coefficient (ADC) images were generated automatically on the MR console system using a monoexponential ADC model for all three b-values.

CT imaging technique

CT examinations were performed using a 2 × 128 row detector CT scanner (Somatom Definition Flash; Siemens Healthcare, Erlangen, Germany), a 128-row detector CT scanner (Somatom Definition AS; Siemens Healthcare, Erlangen, Germany), and a 320-detector row CT scanner (Aquilion ONE; Canon Medical Systems, Otawara, Japan).

Axial CT images (120 kVp; 200–750 mAs, adjusted according to patient size; slice thickness, 0.625 mm; table speed, 40 mm per rotation; pitch, 0.987) were acquired after contrast material injections, including late hepatic arterial phase (20–30 s), PVP (60 s), and delayed phase (80 s) after contrast agent administration. All images were reconstructed with a section thickness of 5 mm.

Observation registration

One board-certified abdominal radiologist with 6 years of experience in liver MRI, who was aware of patient clinical information, retrospectively reviewed the MRI and reports in a picture archiving and communication system identifying consecutive observations meeting the inclusion and exclusion criteria. When a target patient was identified, the size and location of individual observations were recorded based on imaging features, and the five largest observations (if >5) were selected for inclusion. After inclusion, one board-certified radiologist with >10 years of experience in MRI reviewed and verified the observations.

Imaging analysis

Two board-certified abdominal radiologists (6 years and 20 years of experience in liver MRI) performed image analysis according to the following steps and were blinded to the final diagnosis. First, two readers assessed the presence or absence of all major features (APHE, enhancing capsule, and washout) and indicated the application of ancillary features (absent, favoring benignity, favoring malignancy or HCC in particular) individually within a week.

Second, immediately after an individual assessment, washout appearance was analyzed using dynamic-enhanced CT imaging.

All discordant imaging features were discussed to achieve consensus imaging features in two separate sessions spaced apart by a week and assigned a final LI-RADS category.

Based on the results of the image review regarding the signal intensity of liver lesions on the PVP and HBP on gadoxetic acid-enhanced liver MRI with PVP and delayed phase on enhanced liver CT, three different imaging criteria for washout were applied as follows: hypointensity on the PVP at gadoxetic acid-enhanced MRI (Criteria 1), hypointensity on PVP at gadoxetic acid-enhanced MRI and/or hypoattenuation on the PVP/delayed phase at dynamic CT (Criteria 2), and hypointensity on the PVP and/or HBP at gadoxetic acid-enhanced MRI (Criteria 3).

Reference standard

All observations included in the study were confirmed by pathological diagnosis or follow-up imaging. As defined in,LI-RADS v. 2018 a lesion was considered benign in the following cases: (i) observations that did not change in size or additional imaging features over 2 years of follow-up (stable) and (ii) observations that reduced in size or disappeared during imaging follow-up (regression). Cases considered as HCC were as follows: (i) pathologically confirmed observations by surgery or biopsy and (ii) observations that increased in diameter ≥50% within 6 months (threshold growth) and definite HCC (progression) at imaging follow-up (LR-5).

When an observation was suspected to be HCC, stable observations after locoregional therapy without pathologic diagnosis were excluded.

Statistical analyses

Interreader agreement of each criteria were assessed using Cohen's κ statistics. Per-lesion sensitivity, specificity, positive-predictive value (PPV), negative-predictive value (NPV), and accuracy were calculated for each imaging diagnostic criterion for HCC. Subsequently, the lesion sensitivity, specificity, and accuracy for the diagnosis of HCC were compared using Pearson's χ^2 test. Diagnostic performance of each criteria were also compared with using binary logistic regression analysis. A p-value < 0.05 was considered statistically significant. Statistical

Table 1. Characteristics of the study population.

Variables	Male (n = 127)	Female (n = 35)	Total (n = 162)
Age, years			
Mean ± SD	64.7 ± 9.2	68.1 ± 9.6	65.5 ± 9.4
Range	37–82	49–87	37–87
Etiology of cirrhosis, n (%)			
HBV	45 (35.4)	15 (42.9)	59 (36.6)
HCV	25 (19.7)	11 (31.4)	34 (21.1)
Alcohol	28 (22.0)	2 (5.7)	29 (18.0)
HBV + HCV	3 (2.4)	1 (2.9)	4 (2.5)
Alcohol + HBV	19 (15.0)	-	19 (11.8)
Alcohol + HCV	7 (5.5)	1 (2.9)	8 (5.0)
Alcohol + HBV + HCV	1 (0.8)	-	1 (0.6)
Autoimmune hepatitis	-	2 (5.7)	2 (1.2)
Polycythemia vera	1 (0.8)	-	1 (0.6)
Cryptogenic	1 (0.8)	3 (8.6)	4 (2.5)
MELD score			
Mean ± SD	9.9 ± 3.5	9.4 ± 2.3	9.8 ± 3.3
Range	6–30	7–17	6–30

HBV, hepatitis B virus; HCV, hepatitis C virus; SD, standard deviation, MELD, model for end-stage liver disease

analyses were performed using the Statistical Package for the Social Sciences (SPSS) (v. 23.0, IBM SPSS Statistics for Windows, Armonk, NY).

RESULTS

The interreader agreement was almost perfect in all washout criteria (Criteria 1, κ = 0.859; Criteria 2, κ = 0.870, Criteria 3, κ = 0.918). The final study population comprised 162 (127 male and 35 female) patients with a mean age of 63.8 ± 8.9 (range: 37–87) years. The characteristics of the study population are shown in Table 1.

Observation characteristics

A total of 226 observations were included in the study, with a mean diameter of 12.3 ± 5.4 (range: 5–37) mm and an average of 1.4 ± 0.8 (range: 1–5) observations per patient [one observation (n = 117), two observations (n = 35), three observations (n = 10), four observations (n = 1), and five observations (n = 1).

Of the 226 observations, 28 (12.4%) were categorized as LR-3. Of these, 12 observations were diagnosed as HCC (5 were by surgery, 3 were by biopsy, and 4 were by imaging follow-up with threshold growth), and 16 were diagnosed as benign (2 were by surgery, 2 were by biopsy, and 12 were by imaging follow-up with stable). Remaining 198 (87.6%) observations were categorized as LR-4. Of these, 124 observations were diagnosed as HCC (52 were by surgery, 9 were by biopsy, and 63 were by imaging follow-up with threshold growth), and 74 were diagnosed as benign (4 were by surgery, 11 were by imaging follow-up with regression, and 59 were by imaging follow-up with stable). The time interval between imaging and diagnosis of all observations was 433.5 ± 349.3 days (range 11–1694); HCC was 262.7 ± 216.3 days (range 11–704), and benign nodule was 808.8 ± 396.5 (range 15–1694). The characteristics of the observations are shown in Table 2.

Frequency of washout according to different washout criteria

Among the LR-3 and LR-4 observations evaluated, hypointensities to the surrounding hepatic parenchyma were observed in 43.4% (98/226) on PVP at MRI (Criteria 1), 67.2% (152/226) on PVP on MRI and/or PVP or delayed phase at CT (Criteria 2), and 87.6% (198/226) on PVP and/or HBP at MRI (Criteria 3). The incidence of APHE in each criteria group was 13.2% (13/98) in Criteria 1, 44.1% (67/152) in Criteria 1, and 57.1% (113/198) in Criteria 3.

Diagnostic performances of different washout criteria

The sensitivity, specificity, PPV, NPV, and accuracy of each imaging criterion are listed in Table 3. Logistic regression analysis revealed that Criteria 1 (p = 0.000) and Criteria 2 (p = 0.030) were statistically significant.

Comparison and statistical significance of sensitivity, specificity, and accuracy by each washout criteria are shown in Table 4. Among the diagnostic criteria, Criteria 2 and 3 showed significantly higher sensitivities for HCC (67.29 and 97.52%, respectively) than Criteria 1 (35.51%) (p < 0.001). Regarding specificity, Criteria 1 (40.74%) and 2 (36.3%) had significantly higher specificities than Criteria 3 (12.96%). There was no significant difference between the specificity of Criteria 1 and 2 (p = 0.427). On

Table 2. Characteristics of the observations.

Variables	HCC (n = 136)	Benign (n = 90)	Total (n = 226)
Size, mm			
Mean ± SD	12.4 ± 5.3	10.5 ± 6.6	12.3 ± 5.4
Range	5–37	7–33	5–37
LI-RADS category			
MF only, n (%)			
LR-3	93 (68.4)	63 (70.0)	156 (69.1)
LR-4	43 (31.6)	27 (30.0)	70 (30.9)
Final category with MF and AF, n (%)			
LR-3	12 (8.8)	16 (17.8)	28 (12.4)
LR-4	124 (91.2)	74 (82.2)	198 (87.6)
Reference standard, n (%)			
Surgery	57 (41.9)	6 (6.7)	63 (27.9)
Biopsy	12 (8.8)	2 (2.2)	14 (6.2)
Threshold growth a	67 (49.3)	-	67 (29.6)
Regression b	-	11 (12.2)	11 (4.9)
Stable c	-	71 (78.9)	71 (31.4)
Time interval between MR imaging and diagnosis, days			
Mean ± SD	262.7 ± 216.3	808.8 ± 396.5	433.5 ± 349.3
Range	11–704	15–1694	11–1694

HCC, hepatocellular carcinoma; SD, standard deviation; LI-RADS, Liver Imaging-Reporting and Data System; MF, major imaging feature; AF, ancillary imaging feature

[a]Observations that increased in diameter ≥50% within 6 months or definite HCC.

[b]Observations that did not change in size or additional imaging features over 2 years of follow-up.

[c]Observations that reduced in size or disappeared during imaging follow-up.

accuracy, Criteria 2 (59.9%) and 3 (65.84%) showed significantly higher than Criteria 1 (37.27%) (p = 0.026 and p = 0.000, respectively). There was no significant difference between the accuracy of Criteria 2 and 3 (p = 0.156).

Compared to Criteria 1 and 3, Criteria 2 was more capable of reducing the number of false-positive diagnoses of HCC with increased sensitivity. In addition, the accuracy of Criteria 1 was significantly lower than those of Criteria 2 and 3. Figure 2 is an example of HCC with washout at Criteria 2 only. Figure 3 shows example of HCC with washout at Criteria 2 and 3.

DISCUSSION

As manifested in the HCC diagnosis guidelines of more than 20 organizations, whether emphasis should be placed on sensitivity or specificity in the diagnosis of HCCs can be influenced by the practice patterns of different geographic areas.[7] At present,LI-RADS v. 2018 recommends that washout should be determined at the PVP of gadoxetic acid-enhanced MRI and states several HBP findings as only ancillary features.[8–10]

Table 3. Diagnostic performances and logistic regression analysis by washout criteria

WO criteria	SS (%)	SP (%)	PPV (%)	NPV (%)	AC (%)	Logistic regression analysis	
						Odds ratio (95% CI)	p-value
Criteria 1[a]	35.51	40.74	54.29	24.18	37.27	0.12 (0.04 ~ 0.39)	0.000
Criteria 2[b]	67.29	36.33	66.67	33.96	59.90	3.80 (1.14 ~ 12.65)	0.030
Criteria 3 ***	95.52	12.96	67.81	46.67	65.84	2.79 (0.84 ~ 9.31)	0.094

AC, accuracy; CI, confidence interval; NPV, negative-predictive value; PPV, positive-predictive value; SP, specificity; SS, sensitivity;WO, washout.

[a]Hypointensity on portal venous phase at MRI.

[b]Hypointensity on portal venous phase at MRI and/or hypoattenuation on portal venous or delayed phase at CT.

[c]Hypointensity on portal venouse phase and/or hepatobiliary phase at MRI.

Table 4. Comparison of sensitivity, specificity, and accuracy by washout criteria

	Sensitivity		
Washout criteria	Difference (95% CI)	χ^2	*p*-value
Criteria 1 *vs* Criteria 2	31.78 (18.50 ~ 43.50)	21.529	**<0.0001**
Criteria 1 *vs* Criteria 3	60.01 (48.98 ~ 68.82)	84.878	**<0.0001**
Criteria 2 *vs* Criteria 3	28.23 (18.26 ~ 37.93)	28.035	**<0.0001**
	Specificity		
Washout criteria	Difference (95% CI)	χ^2	*p*-value
Criteria 1 *vs* Criteria 2	7.41 (−10.55 ~ 24.72)	0.63	0.427
Criteria 1 *vs* Criteria 3	27.78 (11.14 ~ 42.59)	10.511	**0.001**
Criteria 2 *vs* Criteria 3	20.37 (4.42 ~ 35.20)	6.240	**0.013**
	Accuracy		
Washout criteria	Difference (95% CI)	χ^2	*p*-value
Criteria 1 *vs* Criteria 2	18.63 (2.32 ~ 33.46)	4.969	**0.026**
Criteria 1 *vs* Criteria 3	28.57 (12.79 ~ 42.47)	12.587	**0.000**
Criteria 2 *vs* Criteria 3	9.94 (−3.67 ~ 23.18)	2.016	0.156

CI, confidence interval.

Accordingly, recent studies on the application of LI-RADS on gadoxetic acid-enhanced MRI have demonstrated a high specificity (>95%), although they showed a relatively lower sensitivity in the range of 57.3–64% for the diagnosis of HCCs.[11–14] Although LI-RADs had high diagnostic performance in the characterization of lesions larger than 20 mm with major image features, diagnostic challenges with potential failure rates of 30–70% remain in the assessment of lesions in LR-3 and LR-4.[15–17]

Prior studies[18–20] have shown that MRI with hepatobiliary contrast agents may have significantly higher sensitivity than dynamic CT and MRI with extracellular agents for the diagnosis of HCC. Unfortunately, along with increased sensitivity, the use

Figure 2. A 67-year-old male with hepatitis B-related liver cirrhosis. (a) Axial T_2 weighted image and (b) axial T_1 weighted image reveal an ill-defined observation (18 mm in size) in the segment VIII (arrows) with moderate hyperintensity in T_2 weighted image and subtle hypointensity in T_1 weighted image. Gadoxetic acid-enhanced (c) arterial, (d) portal venous, (e) transitional, and (f) HBP images show arterial hyperenhancement, no washout, and ambiguous HBP hypointensity. (g) Diffusion-weighted image (b-value of 800 s/mm2) shows hyperintensity of observation compared to the background liver. The final LI-RADS category was determined to be LR-4 according to.LI-RADS v. 2018 On dynamic CT, arterial enhancement and washout appearance are noted at the same observation in (h) arterial, (i) portal venous, and (j) delayed phase. This observation was removed by surgical resection and confirmed as hepatocellular carcinoma. HBP, hepatobiliary phase; LI-RADS, Liver Imaging Reporting and Data System.

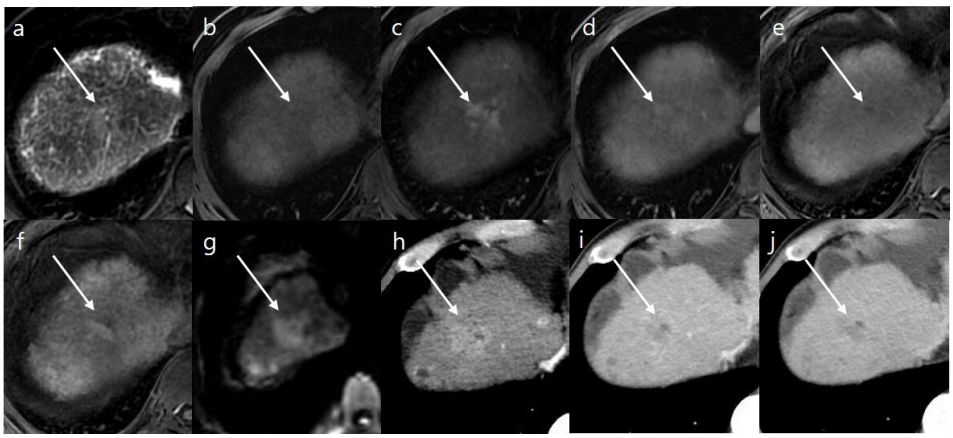

Figure 3. A 64-year-old female with hepatitis B-related liver cirrhosis. (a) Axial T_2 weighted image and (b) axial T_1 weighted image reveal a 10-mm-sized observation in segment VII (arrows) with mild to moderate hyperintensity in T_2 weighted image and hypointensity in T_1 weighted image. Gadoxetic acid-enhanced (c) arterial, (d) portal venous, (e) transitional, and (f) HBP images show arterial hyperenhancement, no washout, subtle hypointensity in transitional phase, and HBP hypointensity. (g) Diffusion-weighted image (b-value of 800 s/mm^2) shows subtle hyperintensity of observation compared to the background liver. The final LI-RADS category was determined to be LR-4 according to.LI-RADS v. 2018. On dynamic CT, arterial enhancement and washout appearance are noted at the same observation in (h) arterial, (i) portal venous, and (j) delayed phase. Using liver transplantation, this observation was confirmed as hepatocellular carcinoma. HBP, hepatobiliary phase; LI-RADS, Liver Imaging Reporting and Data System

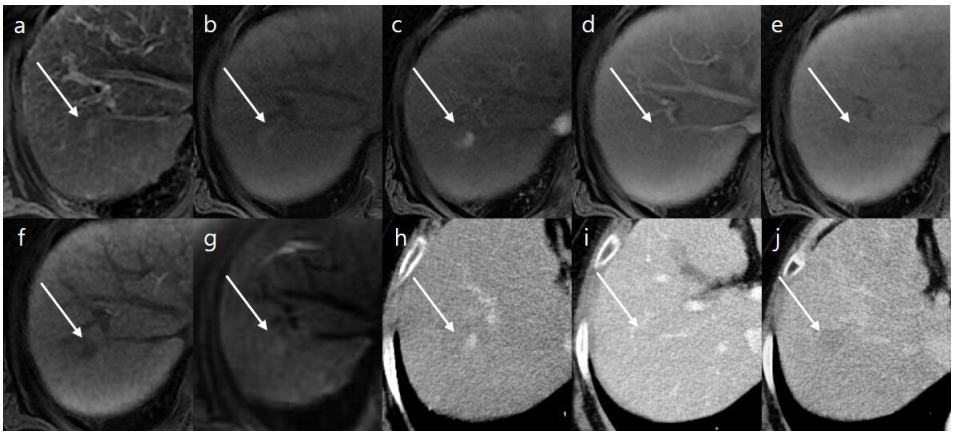

of hepatobiliary contrast agents may decrease specificity. This means that hepatobiliary agents induce parenchymal enhancement in the TP and HBP and obscure the distinction. These facts were the basis for the rigorous application of the concept of washout in LI-RADS.

Even in our study, although HBP hypointensity showed significantly high sensitivity in nodules with uncertainty such as LR-3 or LR-4, the specificity for HCC was low at 13%, making it difficult to accept as a major image feature that can replace washout.

According to Corwin,[21] the LI-RADS categories differ between CT and MRI for 77.2% of observations, and approximately half of the patients receive both CT and MRI. Up to 2% of the observations are observed on CT alone.

Our data showed that the frequency of washout increased from 43.5% in PVP on MRI to 67.1% in PVP on MRI or CT among the LR-3 and LR-4 groups. Although there is no washout at PVP on MRI, the sensitivity could be increased from 35 to 67% without loss of specificity in the actual diagnosis using CT image checking for washout. Therefore, in this case, we could improve the accuracy of the HCC diagnosis of uncertain nodules.

This study has several limitations. First, the study was conducted retrospectively at a single institution, which could have led to selection bias. The overall diagnostic performance may be lower than that of conventional LI-RADS studies since LR-5 was excluded from our study population. We selected patients who have had CT and MRI within 2 weeks only, there are many cases that are not confirmed HCC before surgery or are not definite HCC on CT, so selecting a case may not represent general LR3 or LR4. Second, confirmation of many observations was made by subsequent imaging, which is an inevitable limitation because subsequent imaging is generally favored at this stage, rather than pathological diagnosis. However, the reference standard was strictly applied, and only cases with evident imaging features in subsequent imaging were included in this study population. Third, the final diagnosis was divided into HCC and benign lesion. Although LR-M was excluded from this study, it was possible that unconfirmed non-HCC lesions were included in the HCC category.

Our results may provide preliminary evidence to justify the inclusion of CT images for mandatory upgrades to LR-3 and LR-4 observations that have no washout at PVP on MRI. The proposed change to the current diagnostic algorithm may be clinically important, resulting in more aggressive management or decreasing imaging follow-up for intermediate observations.

In conclusion, although the LI-RADS lexicon does not permit the interchange or combined use of image modalities, complementary use of dynamic CT on the basis of gadoxetic acid-enhanced MRI may helpful in evaluating washout appearance as a major imaging feature.

FUNDING

This study was supported by Dong-A university research fund.

REFERENCES

1. Cancer Today: World Health Organization. 2018. Available from: https://gco.iarc.fr/today/online-analysis-table?v=2018&mode=cancer&mode_population=continents&population=900&populations=900&key=asr&sex=0&cancer=39&type=1&statistic=5&prevalence=0&population_group=0&ages_group%5B%5D=0&ages_group%5B%5D=17&group_cancer=1&include_nmsc=1&include_nmsc_other=1
2. Liver Imaging Reporting and Data System version 2018: American College of Radiology. 2018. Available from: https://www.acr.org/-/media/ACR/Files/RADS/LI-RADS/LI-RADS-2018-Core.pdf?la=en
3. Tang A, Cruite I, Mitchell DG, Sirlin CB. Hepatocellular carcinoma imaging systems: why they exist, how they have evolved, and how they differ. *Abdom Radiol (NY)* January 2018; **43**: 3–12. https://doi.org/10.1007/s00261-017-1292-3
4. Kudo M, Matsui O, Izumi N, Iijima H, Kadoya M, Imai Y, et al. JSH consensus-based clinical practice guidelines for the management of hepatocellular carcinoma: 2014 update by the liver cancer study group of japan. *Liver Cancer* 2014; **3**: 458–68. https://doi.org/10.1159/000343875
5. Elsayes KM, Hooker JC, Agrons MM, Kielar AZ, Tang A, Fowler KJ, et al. 2017 version of li-rads for ct and mr imaging: an update. *Radiographics* 2017; **37**: 1994–2017. https://doi.org/10.1148/rg.2017170098
6. Joo I, Kim H, Lee JM. Cancer stem cells in primary liver cancers: pathological concepts and imaging findings. *Korean J Radiol* 2015; **16**: 50–68. https://doi.org/10.3348/kjr.2015.16.1.50
7. Seale MK, Catalano OA, Saini S, Hahn PF, Sahani DV. Hepatobiliary-specific mr contrast agents: role in imaging the liver and biliary tree. *Radiographics* 2009; **29**: 1725–48. https://doi.org/10.1148/rg.296095515
8. Hecht EM, Holland AE, Israel GM, Hahn WY, Kim DC, West AB, et al. Hepatocellular carcinoma in the cirrhotic liver: gadolinium-enhanced 3d t1-weighted mr imaging as a stand-alone sequence for diagnosis. *Radiology* 2006; **239**: 438–47. https://doi.org/10.1148/radiol.2392050551
9. Piana G, Trinquart L, Meskine N, Barrau V, Beers BV, Vilgrain V. New mr imaging criteria with a diffusion-weighted sequence for the diagnosis of hepatocellular carcinoma in chronic liver diseases. *J Hepatol* 2011; **55**: 126–32. https://doi.org/10.1016/j.jhep.2010.10.023
10. Shankar S, Kalra N, Bhatia A, Srinivasan R, Singh P, Dhiman RK, et al. Role of diffusion weighted imaging (dwi) for hepatocellular carcinoma (hcc) detection and its grading on 3t mri: a prospective study. *J Clin Exp Hepatol* 2016; **6**: 303–10. https://doi.org/10.1016/j.jceh.2016.08.012
11. Joo I, Lee JM, Lee DH, Ahn SJ, Lee ES, Han JK. Liver imaging reporting and data system v2014 categorization of hepatocellular carcinoma on gadoxetic acid-enhanced mri: comparison with multiphasic multidetector computed tomography. *J Magn Reson Imaging* March 2017; **45**: 731–40. https://doi.org/10.1002/jmri.25406
12. Allen BC, Ho LM, Jaffe TA, Miller CM, Mazurowski MA, Bashir MR. Comparison of visualization rates of li-rads version 2014 major features with iv gadobenate dimeglumine or gadoxetate disodium in patients at risk for hepatocellular carcinoma. *AJR Am J Roentgenol* 2018; **210**: 1266–72. https://doi.org/10.2214/AJR.17.18981
13. Kim YY, An C, Kim S, Kim MJ. Diagnostic accuracy of prospective application of the liver imaging reporting and data system (li-rads) in gadoxetate-enhanced mri. *Eur Radiol* 2018; **28**: 2038–46. https://doi.org/10.1007/s00330-017-5188-y
14. Choi SH, Byun JH, Lim YS, et al. Liver imaging reporting and data system: patient outcomes for category 4 and 5 nodules. *Invest Radiol* 2018; **51**: 483–90. https://doi.org/10.1097/RLI.0000000000000258
15. Ronot M, Fouque O, Esvan M, Lebigot J, Aubé C, Vilgrain V. Comparison of the accuracy of aasld and li-rads criteria for the non-invasive diagnosis of hcc smaller than 3 cm. *J Hepatol* April 2018; **68**: S0168-8278(17)32529-1: 715–23: . https://doi.org/10.1016/j.jhep.2017.12.014
16. Cha DI, Jang KM, Kim SH, Kang TW, Song KD. Liver imaging reporting and data system on ct and gadoxetic acid-enhanced mri with diffusion-weighted imaging. *Eur Radiol* 2017; **27**: 4394–4405. https://doi.org/10.1007/s00330-017-4804-1
17. Liu W, Qin J, Guo R, Xie S, Jiang H, Wang X, et al. Accuracy of the diagnostic evaluation of hepatocellular carcinoma with li-rads. *Acta Radiol* 2018; **59**: 140–46. https://doi.org/10.1177/0284185117716700
18. Renzulli M, Biselli M, Brocchi S, Granito A, Vasuri F, Tovoli F, et al. New hallmark of hepatocellular carcinoma, early hepatocellular carcinoma and high-grade dysplastic nodules on gd-eob-dtpa mri in patients with cirrhosis: a new diagnostic algorithm. *Gut* September 2018; **67**: 1674–82. https://doi.org/10.1136/gutjnl-2017-315384
19. Roberts LR, Sirlin CB, Zaiem F, Almasri J, Prokop LJ, Heimbach JK, et al. Imaging for the diagnosis of hepatocellular carcinoma: a systematic review and meta-analysis. ; January 2018, pp.401–21. https://doi.org/10.1002/hep.29487
20. Choi SH, Lee SS, Park SH, Kim KM, Yu E, Park Y, et al. LI-rads classification and prognosis of primary liver cancers at gadoxetic acid-enhanced mri. *Radiology* February 2019; **290**: 388–97. https://doi.org/10.1148/radiol.2018181290
21. Corwin MT, Fananapazir G, Jin M, Lamba R, Bashir MR. Differences in liver imaging and reporting data system categorization between mri and ct. *AJR Am J Roentgenol* 2016; **206**: 307–12. https://doi.org/10.2214/AJR.15.14788